THE BALTIC JOURNAL
OF ROAD AND BRIDGE ENGINEERING

2008
3(4): 181–186

EFFECTS OF TIRE INFLATION PRESSURE AND LOAD ON PREDICTED PAVEMENT STRAINS

Dae-Wook Park[1], Amy Epps Martin[2], Jin-Hoon Jeong[3], Seung-Tae Lee[4]

[1, 4] *Dept of Civil Engineering, Kunsan National University, San 68 Miryong-dong, Kunsan, Chellabuk-do, 573-701, Korea, e-mails:* [1] *dpark@kunsan.ac.kr;* [4] *stlee@kunsan.ac.kr*
[2] *Texas A&M University System, 503F, 3135 TAMU, College Station, Texas 77843-3135, USA E-mail: a-eppsmartin@tamu.edu*
[3] *Dept of Civil Engineering, Inha University, 253 Yonghyun-Dong, Nam-Gu, Incheon, 402-751, Korea E-mail: jhj@inha.ac.kr*

Abstract. In this paper, effects of tire loads and inflation pressures on predicted pavement responses were presented. The objective was to study the effect of increased tire loads and tire inflation pressures on predicted transverse strains and vertical strains at the different pavement layers and material properties. A 3 dimensional (3D) tire contact stresses for 6 different tires were interpolated from the database of the measured tire contact stresses. The shape of measured tire contact stresses is dependent on tire loading conditions. The results show that the predicted values were different near the asphalt concrete (AC) layer by increased tire inflation pressure. Under the increased tire load, the predicted values were different at the base and subgrade layer. From statistical analysis, predicted transverse strains at the bottom of asphalt layer and vertical strains at the top of subgrade are affected by different AC thicknesses, AC moduli, and subgrade moduli.

Keywords: 3D tire contact stress, tire inflation pressure, tire load, 3D finite element analysis, predicted pavement strain.

1. Introduction

Recently, the tire inflation pressure has been significantly increased compared to that of 1960 and 1970. Also, the permitted tire load has been significantly increased. Generally, higher tire loads require higher inflation pressures to maintain optimal tire performance. The recommended pressures are typically 620–793 kPa, with reaching as high as 896 to 1000 kPa in certain applications. As tire loads and inflation pressure have been increased, tire types are shifted from bias ply tire to radial tire or wide base tire. The increased tire loads and inflation pressures caused the premature failure of pavements. Pavement designers have used uniform and circular distributed tire inflation pressures instead of tire contact stresses that have been believed as more realistic phenomena of tire and pavement interactions.

Wang and Machemehl (2006) conducted the prediction of pavement response using measured tire contact stresses. The results of a 3 dimensional (3D) finite element model (FEM) with measured tire contact stresses were compared with those of a layered elastic program. The results from the layered elastic program showed that a circular uniform pressure distribution overestimated tensile strains at the bottom of the asphalt layer and overestimated compressive strains at the top of the subgrade. They also studied the effects of tire pressures on pavement response, and found that increased tire pressure can cause more fatigue cracking and rutting. Park *et al.* (2005b) conducted an analysis of the pavement response of WesTrack. The profiles of permanent deformation at WesTrack were simulated by elastic-viscoplastic constitutive model embedded in 3D FEM and measured tire contact stresses. They also investigated the effect of tire load on pavement response. They found that the tire pressure distribution was found to be dependent on the tire load, and it had significant influence on the distributions of shear stress and plastic strain. Under the fixed tire pressure, the increased shear stresses and plastic strains were found at the tire edges. The finite element (FE) analysis based on the elastic-viscoplastic relation was able to simulate the measured permanent deformation profiles. De Beer *et al.* (1997, 2002; De Beer, Fisher 1997) conducted analysis of the measured contact stresses using by the Vehicle-Road Surface Pressure Transducer Array (VRSPTA). They found that the measured max vertical stresses are 1 to 2 times higher than designated tire inflation pressures around the edges of the contact area, particularly in the shoulder areas at the either side, due to the bending stiffness of the side walls and tread band. These observations indicated that current design assumptions might lead to pavements that are inadequate to carry the expected wheel load applications over the design life.

ISSN 1822-427X print / ISSN 1822-4288 online DOI: 10.3846/1822-427X.2008.3.181-186
http://www.bjrbe.vgtu.lt

In this paper, the effects of tire load and inflation pressure on pavement response were investigated. The pavement response was predicted at the bottom of asphalt layer and at the top of subgrade layer. The increased tire loads were applied at the constant tire inflation pressure and the increased tire inflation pressures were applied at the constant tire load. A 3D FE analysis under 3D tire contact stresses was used to investigate the pavement response. 6 different tires and 2 different pavement structures were used to investigate the effects of tire loading conditions on pavement response.

2. Distributions of tire contact stresses

In this section, the loading conditions of 6 different tires used in this study are described. The measurement of tire contact stresses is explained briefly. The analysis of the measured tire contact stresses was conducted to investigate the effects of tire inflation pressures and loads on the contact stress distributions. The data of measured contact stresses were too fine to apply 3D FEM; therefore the procedures of data processing of tire contact stresses which can be feasibly applied the 3D FEM.

The 3D tire contact stresses, which are longitudinal, transverse, and vertical ones, on the 295/75*R*22.5 radial, 11*R*22.5 radial, 10×20 Bias Ply, and 425/65*R*22.5 wide-base tires were measured with the VRSPTA in a study conducted in 1997 by the University of California at Berkeley (UCB). The 3D tire contact stresses on 11*R*24.5 and 215/75*R*17.5 low profile radial tires were measured with the SIM Mk IV system in a research project conducted by the Texas Transportation Institute (TTI). The descriptions of the VRSPTA systems and the Stress-In-Motion (SIM) Mk IV system can be referenced by de Beer and Fisher (1997; 2002).

2.1. Tire loading conditions

Five different loading conditions were selected to analyze pavement response by 6 different tires. The increased tire inflation pressures were used at the constant tire load and the increased tire loads were applied at the constant tire inflation pressure. The load and tire inflation pressures used in this paper are summarized in Table 1.

The measurements of tire contact stresses were not available for most of loading conditions; therefore the 3D tire contact stresses were obtained by using TireView. TireView is a computer program to estimate tire contact pressure distributions in the longitudinal, lateral, and vertical directions. The program uses an interpolation routine on the database of measured tire contact pressures established to estimate contact stress distributions for a given tire load and tire inflation pressure (Fernando *et al.* 2006). Since the measurement of tire-pavement contact stress for different tires was done at specific intervals of tire load and tire inflation pressure, the authors established a procedure to predict tire contact pressure distributions for any given tire load and tire within the range of the compiled test data.

Based on evaluating a number of curve fitting methods, the authors selected polynomial interpolation as the basis for predicting tire contact stress distributions in the TireView program. Polynomial interpolation can be defined as the act of fitting a given function with defined values in certain discrete data points. This function may actually be any discrete data set (such as obtained sampling), but it is generally assumed that such data may be described by a function. Thus, given n points (x_1, y_1), (x_2, y_2), ..., (x_n, y_n), where $\{x_1, x_2, x_3, \ldots, x_n\}$ are all different, the interpolating polynomial for these n points is a function of the form $p(x) = a_0 + a_1x + a_2x + \ldots + a_nx^n$ such that $p(x_j) = y_j$ for all x_j, $j = 1$ to n. The Lagrange form of the interpolating polynomial satisfying this condition is given by:

$$p(x) = \sum_{j=1}^{n} y_j l_j(x), \tag{1}$$

where $l_j(x) = \prod_{\substack{k=1 \\ k \neq j}}^{n} \frac{x - x_k}{x_j - x_k}$.

In case of $j = 1$, $l_j(x)$ is $\frac{(x - x_2)(x - x_3)}{(x_1 - x_2)(x_1 - x_3)}$ and $p(x_j)$ is y_1.

Numerically, TireView uses Neville's algorithm to construct the Lagrange interpolating polynomial (Press *et al.* 2002). The program does a series of 1-dimensional interpolations in stages to estimate the 3D tire contact stress distributions for a given tire type, tire load, and tire inflation pressure using the data base of measure tire contact stresses.

To gauge the predictive accuracy of the algorithm used in TireView, authors did the predictions for the 11*R*24.5 radial tire without the measured contact forces at the tire load of 27.5 kN and 896 kPa inflation pressure. Fig. 1 shows the biased values between measured and predicted force in z-direction. Considering that the measured contact forces for the cases considered were not used in the prediction, the interpolated force distributions reasonably approx the measured distributions within 3% difference.

Table 1. Summary of load and tire inflation pressure combinations used in analyses

UCB test				TTI test			
295/75*R*22.5; 11*R*22.5; 10×20		425/65*R*22.5		11*R*24.5		215/75*R*17.5	
Load	Pressure	Load	Pressure	Load	Pressure	Load	Pressure
kN	kPa	kN	kPa	kN	kPa	kN	kPa
26	517	37	552	21	483	18	689
26	689	37	689	21	621	18	793
26	820	37	827	21	758	18	896
31	820	44	827	26	758	13	896
36	820	51	827	30	758	22	896

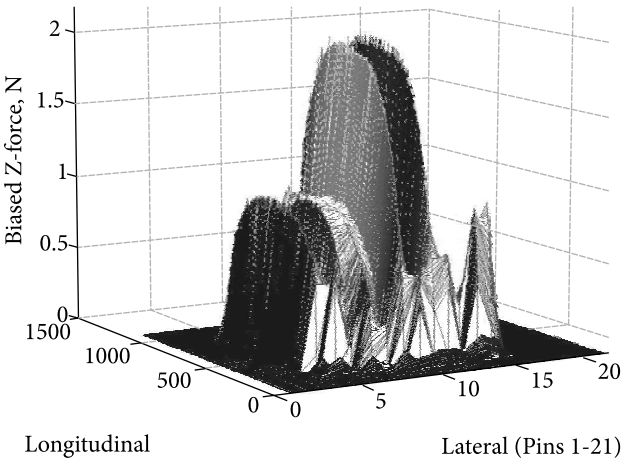

Fig. 1. The biased values between the measured and predicted vertical forces for 11*R*24.5 at 27.5 kN tire load and 896 kPa tire inflation pressure

2.2. Analysis of tire contact stresses

It is well known that the measured contact stresses are higher than the design value of tire inflation pressures. The distributions of tire contact stresses depend on tire type, tire load, and tire inflation pressure. The distributions of tire contact stresses of a 11*R*22.5 radial tire and a 10×20 bias ply tire by different tire load and tire inflation pressure were investigated to analyze the difference of the values and shape of distributions of tire contact stresses.

As shown in Fig. 2, the tire contact stresses at the both edge treads of tire are higher than those of middle treads at the 26 kN tire load and 517 kPa tire inflation pressure for the 11*R*22.5 radial tire. The distributions of tire contact stresses shows as flat at the 26 kN tire load and 689 kPa tire inflation pressure. The tire contact stresses at the middle treads are higher than those of the edge tread at the 26 kN tire load and 820 kPa tire inflation pressure. The tire contact stresses at the both edge treads are higher than those of the middle treads at the 36 kN tire load and 82 kPa tire inflation pressure. At the constant tire load, the distributions of tire contact stresses are changed from higher edge tire contact stresses to higher middle tire contact stresses as tire inflation pressure increases. At the constant tire inflation pressure, the tire contact stresses at the edge area become higher as tire load increases. The similar tends were shown for the 10×20 bias ply tire; however, tire contact stresses for the 11*R*22.5 radial tire are much higher than those of 10×20 bias ply tire at the same designated tire inflation pressure. Considering that the bias ply tires were replaced by the radial tires in almost all countries, current pavement design method which the tire inflation pressure has been used should be reconsidered.

3. The construction of pavement model

A 3D FEM was necessary to investigate pavement response under the 3D tire contact stresses which are contact stresses in transverse, longitudinal, and vertical directions.

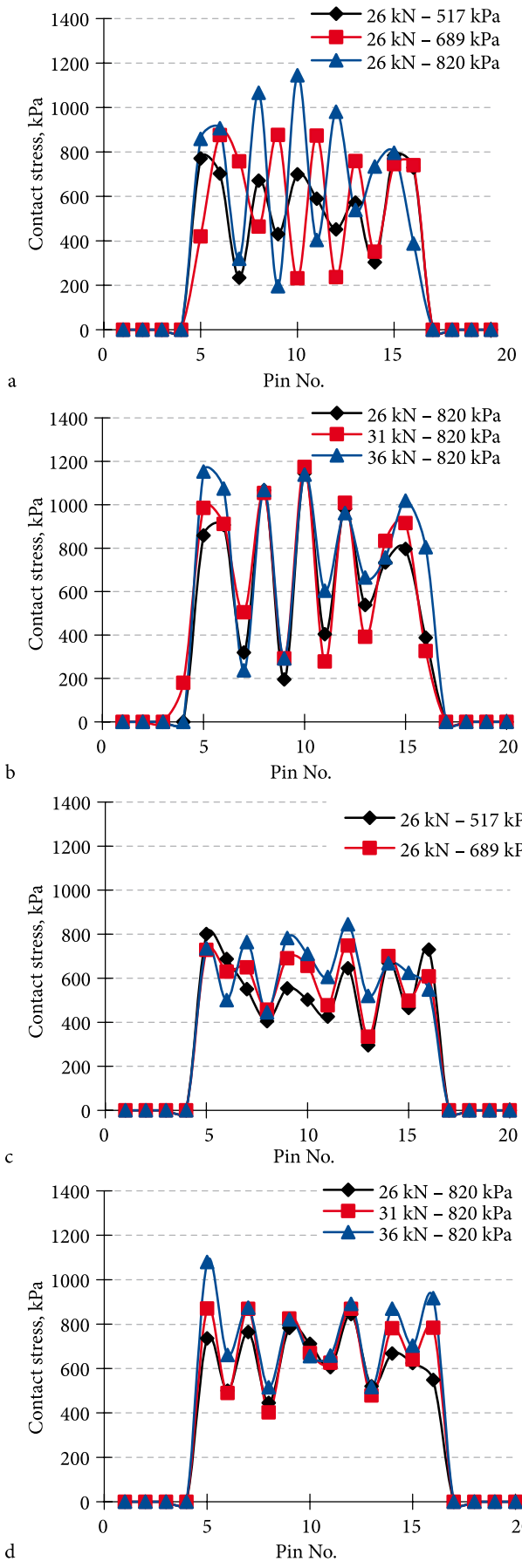

Fig. 2. Distributions of tire contact stresses: a, b – 11*R*22.5 radial tire; c, d – 10×20 bias ply tire

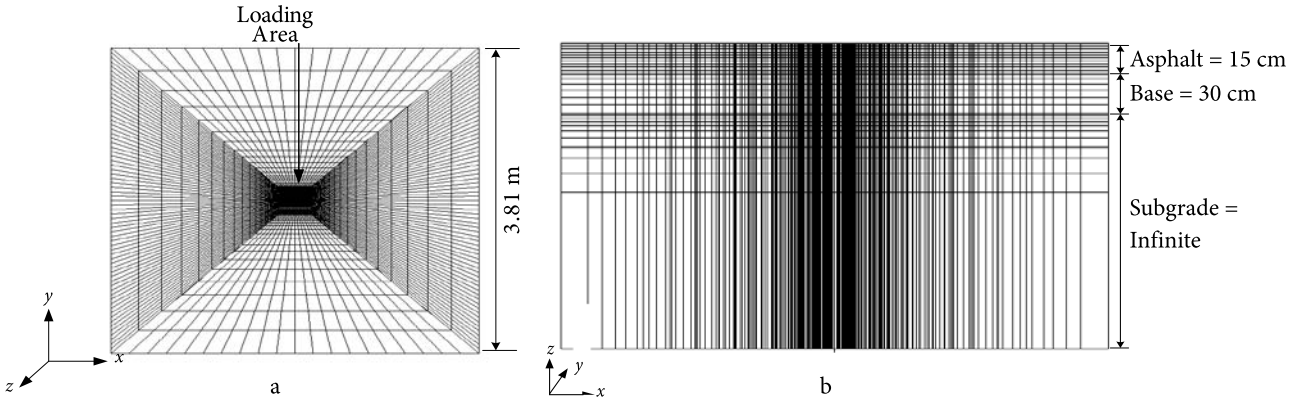

Fig. 3. 3D FEM: a – top view (*y* is in direction of wheel travel); b – vertical view in case of asphalt layer is 15 cm and base layer is 30 cm (Park *et al.* 2005a)

3.1. 3D Finite Element Model (3D FEM)

The authors established a 3D FEM based on the multi-purpose FE package, ABAQUS. Initially, a suitable mesh configuration had to be determined for predicting pavement response under measured tire contact stresses. For this purpose, the authors evaluated a number of mesh configurations of varying number of elements and element types by comparing FE predictions with corresponding predictions from a layered elastic program. The lateral and longitudinal dimensions of the FE mesh were varied until predictions of pavement response, compared reasonably well with the layered elastic analysis results. From this analysis, a FE mesh with lateral and longitudinal dimensions of 3.81 m × 3.81 m was found to be appropriate. In addition, the subgrade was modeled using infinite elements. The asphalt concrete (AC) layers on the top of base layer were varied in the analyses, as shown in Table 2. Two different thickness (50 and 150 cm) of AC layer at a 30 cm base layer were used to study the effect of pavement thickness on pavement response. Fig. 3 shows the 3D FE mesh used in this study. Elements in the region of the tire contact stresses are approx 17 mm (column) × 5 mm (row) in size, with the tire contact area consisting of 20 columns and 68 rows. The elastic modulus of each layer was varied according to Table 2. A Poisson's ratio of 0.4 for all the layers was used.

Table 2. Pavement structures analyzed

Case No.	Layer				
	thickness, cm		modulus of elasticity, MPa		
	asphalt	base	asphalt	base	subgrade
1	5	30	4482	690	52
2	5	30	2758	690	103
3	150	30	2758	690	52
4	150	30	4482	690	103

3.2. Processing the tire contact stress

Tire contact stresses were measured along the longitudinal direction at 0.35 mm intervals for the TTI tests and at approx 2 mm intervals for the UCB tests. These measurements are much too fine to use directly in a 3D FE analysis. To reduce computation time to a feasible level the authors used a simple routine to reduce the sampling rate without significant accuracy loss. When the sampling data is decreased, the process is called decimation because the original data is decimated (Samuel, Ruth 1993). The decimation was accomplished using a procedure that preserves the frequency content of the original data, and resulted in a mesh configuration where the finest mesh size is approx 5 mm (0.2 inch) in the direction of wheel travel. Fig. 4 shows the original and decimated data of vertical tire contact stress for the 11*R*22.5 radial tire which was tested using by UCB tests corresponding to a test inflation pressure of 517 kPa and a tire load of 26 kN, which is the case of overloaded/under an inflation pressure.

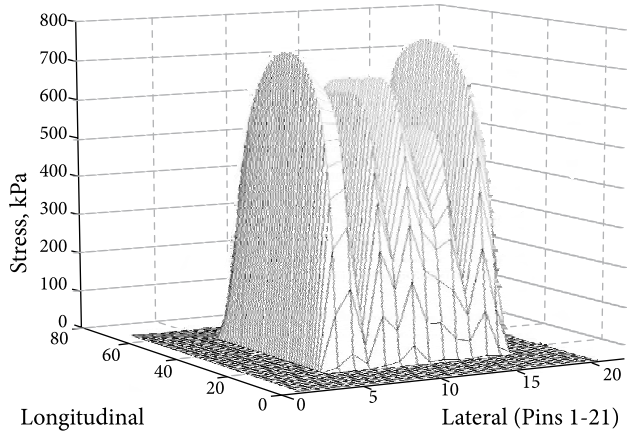

Fig. 4. Decimated vertical tire contact stresses for 11*R*22.5 at 517 kPa inflation pressure and 26 kN tire load

4. Prediction of pavement response

After establishing the model of pavement structures, the analysis using the results of 3D FE analysis under the 3D contact stresses was conducted. The 2 types of loading conditions, which the tire inflation pressures are increased at the constant tire load and the tire load increased at the constant tire inflation pressure, were used to investigate the transverse strain and vertical strains at different depths of pavement structure. To find the critical point for a given condition, the tensile strain at the bottom of the AC layer and the compressive

strain at the top of subgrade were evaluated at the centre and along the 4 edges of the tire contact area. Authors found the predicted response at the centre of the loaded area to be critical. The statistical analysis was conducted to find the effect of transverse and vertical strains at the critical location by different pavement structures and material properties.

4.1. Pavement response

The predicted horizontal and vertical strains from the 3D FE analysis under the 3D tire contact stresses were to investigate the difference between 2 types of loading conditions. The combinations of loading conditions are described in Table 1. Fig. 5 shows the results of transverse and vertical strain using the 11*R*24.5 low profile radial tire. To find the effect of tire inflation pressure on transverse and vertical strain of pavement, the tire inflation pressures at 483, 621, and 758 were used at the 21 kN tire load. To study the effect of tire load, tire loads at 21, 26, and 30 kN were used at 758 kPa. In Figs 5a, 5b the predicted transverse and vertical strain at the bottom of AC layer (= 4.45 cm) and top of base layer are increased as the tire inflation pressure increases and the difference is diminished from the middle of base and to the subgrade layer. In Figs 5c, 5d the predicted transverse and vertical strains show no significant difference at the AC layer, but the predicted strain is increased at the base and subgrade layers as the tire load increases. This finding indicates that the increased tire inflation pressure more likely affects the transverse and vertical strain near the AC surface layer and the increased tire load affects the transverse and vertical strain at the top of subgrade layer. The results also suggest that the effects of the increased tire inflation pressure are mainly seen near the surface layer and diminish with depth and the effects of increased tire load are seen at the bottom layers.

4.2. Statistical analysis of pavement strain results

The authors have conducted an analysis of variance (ANOVA) at a 5% significance level ($\alpha = 0.05$) to examine transverse strains at the bottom of asphalt layer and vertical strains at the top of subgrade layer by different pavement

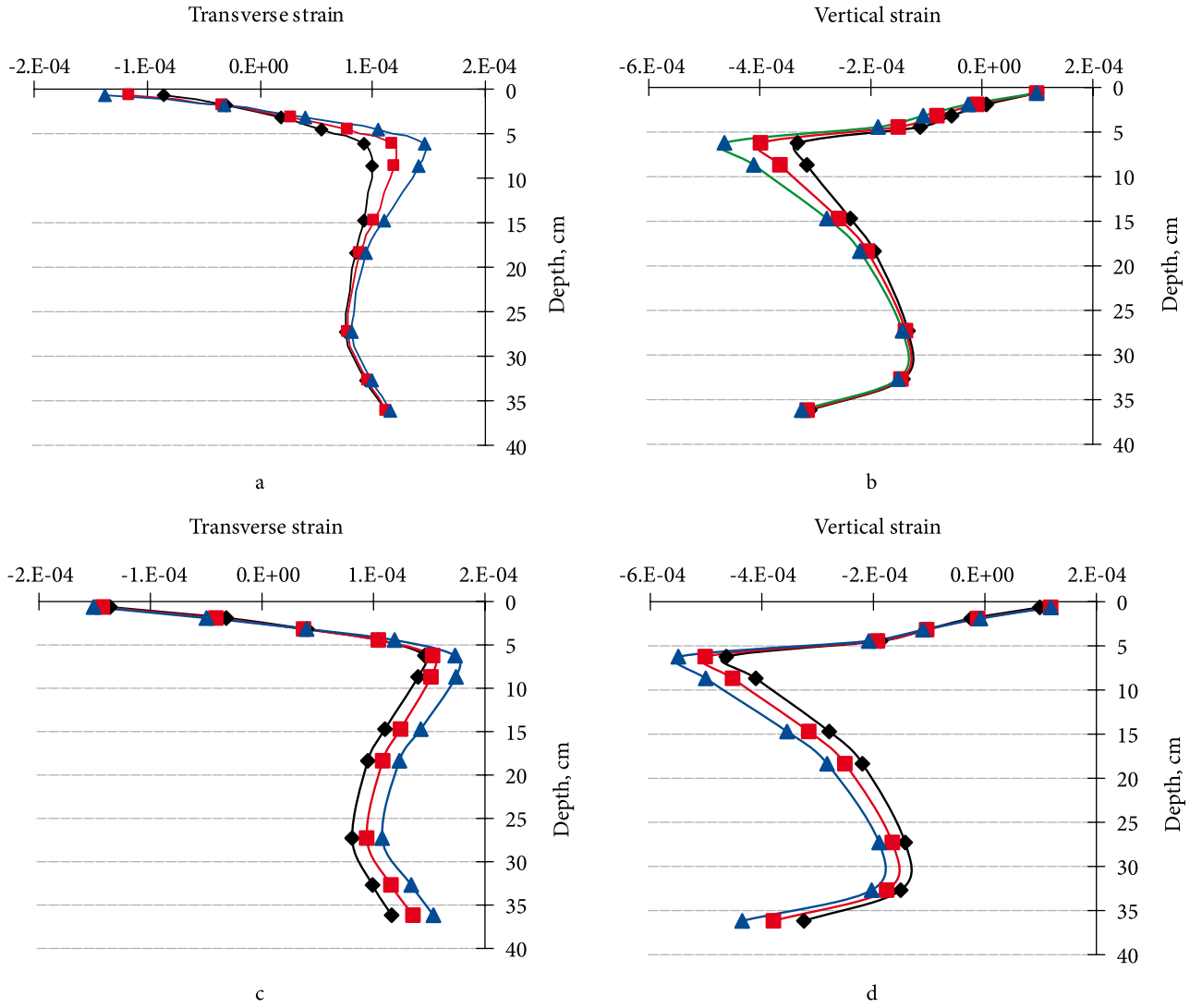

Fig. 5. Predicted transverse and vertical strains for the case 1 of Table 2 by 11*R*24.5 radial tire: a, b – increased tire inflation pressure; c, d – increased tire load (21 kN–758kPa; 26 kN–758kPa; 30 kN–758kPa)

thickness and material properties (Neter *et al.* 1996). Total 120 predicted strains at microstrain were obtained under 6 different tire types, 5 different loading conditions, 2 different pavement thickness, and 2 different material properties. The ANOVA test was performed based on the results obtained by 3 variables (2 AC layer thickness, AC moduli, and subgrade moduli). Results of the ANOVA test are shown in Table 3.

Table 3. The ANOVA test results ($\alpha = 0.05$) for predicted strain

Test option	Predicted strain at microstrain	Test result
AC layer thickness (5 cm, 15 cm)	Transverse strain	H_a ($\varepsilon_{t5} \neq \varepsilon_{t15}$)
	Vertical strain	H_a ($\varepsilon_{v5} \neq \varepsilon_{v15}$)
AC modulus (2578 MPa, 4482 MPa)	Transverse strain	H_a ($\varepsilon_{t2578} \neq \varepsilon_{t4482}$)
	Vertical strain	H_a ($\varepsilon_{v2578} \neq \varepsilon_{v4482}$)
Subgrade modulus (52 MPa, 103 MPa)	Transverse strain	H_a ($\varepsilon_{t52} \neq \varepsilon_{t103}$)
	Vertical strain	H_a ($\varepsilon_{v52} \neq \varepsilon_{v103}$)

For 3 variables tested by ANOVA at a 5% significance level, the results show that the predicted transverse and vertical strains are significantly different for different AC thicknesses, AC moduli, and subgrade moduli. The conclusion based on the results of the limited ANOVA test is that the predicted transverse strains at the bottom of the AC layer and the predicted vertical strains at the top of subgrade are affected by the AC thickness, AC modulus and subgrade modulus.

5. Conclusions

The results of this limited study show that the distribution of contact stresses is different by the combinations of tire loads and tire inflation pressures. At the constant load, the contact stresses of the middle treads are higher than those of the both edge treads as tire inflation pressure increases. At the constant tire inflation pressure, tire contact stresses of the both edge treads are higher than those of the middle treads as tire load increases. In general, the contact stresses are higher than the designated tire inflation pressure. This result indicates that contact stresses between tire and pavement surface should be considered instead of tire inflation pressures during pavement design processes.

The numerical results of 3D FE analysis under different loading conditions showed that the predicted transverse and vertical strain near the AC layer are increased as the tire inflation pressure increases and the difference diminish from the middle of base and to the subgrade layer. The predicted transverse strain and vertical strain show no significant difference at the AC layer, but the predicted strain is increased at the base and subgrade layers as tire load increases. This finding indicates that the increased tire inflation pressure more likely affects the transverse and vertical strain near the AC surface layer and the increased tire load affects the transverse and vertical strain at the top of subgrade layer. The results also suggest that the effects of the increase of tire inflation pressure are mainly seen near the surface layer and diminish with the depth and the effects of increased tire load are seen at the bottom layers.

Comparison of the results from the limited ANOVA test at a 5% confidence level showed that the differences in the predicted transverse strain at the bottom of asphalt layer and the predicted vertical strain at the top of subgrade layer are affected by the AC thickness, AC modulus, and subgrade modulus.

Acknowledgements

This work was supported by the Korea Research Foundation Grant funded by the Korean Government (MOEHRD, Basic Research Promotion Fund) (KRF-2006-003-D00603). The authors would like to thank the MOEHRD for support.

References

De Beer, M.; Fisher, C. [on-line] 1997. *Contact stresses of pneumatic tires measured with the Vehicle-Road Surface Pressure Transducer Array (VRSPTA) system for the University of California at Berkeley (UCB) and the Nevada Automotive Test Center*, Contract Research Report No. CR-97/053 [cited 7 Oct, 2007]. Available from Internet: <http://www.its.berkeley.edu/pavementresearch/PDF/Contact%20Stresses%20of%20Pneum.PDF>.

De Beer, M.; Fisher, C. 2002. *Tire contact stresses of pneumatic tires measured with the stress-in-motion (SIM) Mk IV System for the Texas Transportation Institute (TTI)*, Contract Research Report No. CR-2002/82. Transportek, Pretoria, South Africa. 32 p.

De Beer, M.; Fisher, C.; Jooste, F. 1997. Determination of pneumatic tyre/pavement interface contact stresses under moving loads and some effects on pavements with thin asphalt surfacing layers, in *Proc of the 8th International Conference on Asphalt Pavements*, 10–14 Aug, 1997, Seattle, Washington, USA, 179–227.

De Beer, M.; Fisher, C.; Jooste, F. 2002. Evaluation of non-uniform tyre contact stresses on thin asphalt pavements, in *Proc of the 9th International Conference on Asphalt Pavements* [CD-ROM], 17–22 Aug, 2002, Copenhagen, Denmark. 30 p. ISBN 1874633053.

Fernando, E.; Musani, D.; Park, D.; Wenting, L. [on-line] 2006. *Evaluation of effects of tire size and inflation pressure on tire contact stresses and pavement response*, Research Report No. FHWA/TX-06/0-4361-1 [cited 7 Oct, 2007]. Available from Internet: <http://tti.tamu.edu/documents/0-4361-1.pdf>.

Neter, J.; Kuther, M. H.; Wasserman, W.; Nachtsheim, C. J. 1996. *Applied linear statistical models*. 4th edition. McGraw-Hill/Irwin. 1408 p. ISBN 0256117365.

Park, D. W.; Fernando, E. G.; Leidy, J. 2005a. Evaluation of predicted pavement response with measured tire contact stresses, *Transportation Research Record* 1919: 160–170. DOI: 10.3141/1919-17.

Park, D. W.; Martin, A. E.; Masad, E. 2005b. Effects of nonuniform tire contact stresses on pavement response, *Journal of Transportation Engineering* 131(11): 873–879.

Press, W. H.; Teukolsky, S. A.; Vetterling, T. W; Flannery, B. P. 2002. *Numerical recipes in C++: the art of scientific computing*. 2nd edition. Cambridge University Press. 1002 p. ISBN 0521750334.

Samuel, D. S.; Ruth, A. D. 1993. *Signal processing algorithm in Fortran and C*. 4th edition. Prentice Hall. 331 p. ISBN 0138126941.

Wang, F.; Machemehl, R. B. 2006. Mechanistic-empirical study of effects of truck tire pressure on pavement: measured tire-pavement contact stress data, *Transportation Research Record* 1947: 136–145. DOI: 10.3141/1947-13.

Received 11 Jan, 2008; accepted 24 Oct, 2008